

Ensemble-based Kalman Filters in Strongly Nonlinear Dynamics

Zhaoxia PU*¹ and Joshua HACKER²

¹*Department of Atmospheric Sciences, University of Utah, USA*

²*National Center for Atmospheric Research, USA*

(Received 7 March 2008; revised 10 October 2008)

ABSTRACT

This study examines the effectiveness of ensemble Kalman filters in data assimilation with the strongly nonlinear dynamics of the Lorenz-63 model, and in particular their use in predicting the regime transition that occurs when the model jumps from one basin of attraction to the other. Four configurations of the ensemble-based Kalman filtering data assimilation techniques, including the ensemble Kalman filter, ensemble adjustment Kalman filter, ensemble square root filter and ensemble transform Kalman filter, are evaluated with their ability in predicting the regime transition (also called phase transition) and also are compared in terms of their sensitivity to both observational and sampling errors. The sensitivity of each ensemble-based filter to the size of the ensemble is also examined.

Key words: ensemble Kalman filter, nonlinear, data assimilation, Lorenz model

Citation: Pu, Z. X., and J. Hacker, 2009: Ensemble-based Kalman filters in strongly nonlinear dynamics. *Adv. Atmos. Sci.*, **26**(3), 373–380, doi: 10.1007/s00376-009-0373-9.

1. Introduction

Since Lorenz (1963), scientists in many disciplines have paid a great deal of attention to methods for predicting the evolution of nonlinear systems. Because nonlinear systems are sensitive to initial conditions, accurate initial conditions are necessary and important, but the levels of accuracy needed to make significant gains in prediction skill may be prohibitive. In general, it has been recognized that data assimilation involving strongly nonlinear models is a difficult and unsolved problem (e.g., Miller et al., 1994).

In addition to the fact that measurements of strongly nonlinear systems such as the atmosphere are sparse or inaccurate, data assimilation schemes based on assumptions of linearity may fail to track transitions and diverge from the true state. Moreover, for large applications with real data, this divergence may be difficult to detect if there is no prior estimate of the expected performance. Divergence may also be due to inappropriate system noise or systematic errors in the observations (Verlaan and Heemink, 2001).

In recent years, the ensemble Kalman filter has gained popularity in data assimilation problems due to its simple conceptual formulation and relative ease

of implementation. For instance, compared with the traditional Kalman filter, the ensemble Kalman filter does not require a derivation of tangent linear and adjoint models. Another feature of the ensemble Kalman filter is the availability of the ensemble for estimates of the forecast and analysis error covariances that are consistent with the dynamics of the prescribed model and observation error statistics. The forecast ensemble mean and covariance are used to assimilate observations and compute a new analysis ensemble with appropriate statistics, which can then be used to begin another cycle. The new analysis ensemble can be formed either stochastically (Houtekamer and Mitchell, 1998) or deterministically (e.g., Bishop et al., 2001).

Limitations arise from using a finite-sized ensemble, which limits the number of degrees of freedom used to represent forecast and analysis errors. Ensemble filter implementations also typically account only for initial condition uncertainty, neglecting error due to model deficiencies. The latter is true for any data assimilation systems and is a consequence of the difficulty in characterizing model deficiencies.

In this study we examine four different configurations of ensemble Kalman filters for their ability

*Corresponding author: Zhaoxia PU, Zhaoxia.Pu@utah.edu

to predict a nonlinear dynamic system. The Lorenz-63 model is taken as a testbed for numerical experiments. The specific question addressed is the following: can ensemble-based data assimilation techniques improve the prediction of nonlinear dynamics, especially a phase transition within the nonlinear system? This paper also presents the first study to compare four commonly used ensemble Kalman filters in data assimilation.

2. Ensemble Kalman filter methods

In this section, we briefly describe different implementations of ensemble Kalman filters that have appeared in the literature, and are frequently used for atmospheric analysis and prediction.

2.1 Kalman filter

For a given time t , the basic analysis equation for the Kalman filter can be written as:

$$\mathbf{X}_{a,t} = \mathbf{X}_{b,t} + \mathbf{P}_{f,t} \mathbf{H}^T (\mathbf{H} \mathbf{P}_{f,t} \mathbf{H}^T + \mathbf{R})^{-1} (\mathbf{Y}_t - \mathbf{H} \mathbf{X}_{b,t}) \quad (2.1.1)$$

with the analysis error covariances given as:

$$\mathbf{P}_{a,t} = \mathbf{P}_{f,t} - \mathbf{P}_{f,t} \mathbf{H}^T (\mathbf{H} \mathbf{P}_{f,t} \mathbf{H}^T + \mathbf{R})^{-1} \mathbf{H} \mathbf{P}_{f,t} \quad (2.1.2)$$

where \mathbf{X} and \mathbf{Y} denote the model state vector and observation vector, respectively. The subscripts b and a denote the background (first guess) and analysis model state vector. The \mathbf{H} represents the observation operator, which transforms the model state to the observation vector. The superscript T denotes the transpose of the matrix. The phrase $\mathbf{Y}_t - \mathbf{H} \mathbf{X}_{b,t}$ is called the innovation vector. The weight matrix, $\mathbf{K} = \mathbf{P}_{f,t} \mathbf{H}^T (\mathbf{H} \mathbf{P}_{f,t} \mathbf{H}^T + \mathbf{R})^{-1}$, is also called the Kalman gain matrix.

The $\mathbf{P}_{f,t}$ and \mathbf{R} represent the background error covariance and observational error covariance, respectively. They can be defined as:

$$\mathbf{X}_{b,t} = \mathbf{X}_{tr,t} + \varepsilon_b \quad \mathbf{P}_{f,t} = \langle \varepsilon_b \varepsilon_b^T \rangle, \quad (2.1.3)$$

$$\mathbf{Y}_t = \mathbf{H} \mathbf{X}_{tr,t} + \varepsilon_R \quad \mathbf{R} = \langle \varepsilon_R \varepsilon_R^T \rangle, \quad (2.1.4)$$

where subscript tr denotes the true state and $\langle \cdot \rangle$ denotes the expected value. ε_b and ε_R are the background and observation errors, respectively.

Given a linear dynamical model M written in a temporal discrete form as:

$$\mathbf{X}_{b,t+1} = M(\mathbf{X}_t). \quad (2.1.5)$$

The error covariance equation becomes:

$$\mathbf{P}_{f,t+1} = M \mathbf{P}_{a,t} M^T + \mathbf{Q}, \quad (2.1.6)$$

where the matrix \mathbf{Q} is the error covariance matrix for the model errors, which is typically ignored in practice, although its characterization is an active area of research. M^T is the adjoint operator. The equations (2.1.5) and (2.1.6) are integrated to produce the forecast for $\mathbf{X}_{b,t}$ and $\mathbf{P}_{f,t}$, used in the analysis Eqs. (2.1.1) and (2.2.2).

2.2 Ensemble Kalman Filter (EnKF)

To overcome the fact that the true state \mathbf{X}_{tr} is unknown in many systems, the ensemble Kalman filter (EnKF) was first proposed by Evensen (1994). In the EnKF, the error covariances \mathbf{P}_f is approximated using an ensemble forecast and it is assumed that the ensemble mean is the best estimate of the true state (Evensen, 2003). For notational simplicity, the time t subscript in the previous subsection (2.1) is dropped in all of the following sections; it is assumed unless noted otherwise that we are interested in estimating the state at time t .

$$\begin{aligned} \mathbf{P}_f &= \overline{(\mathbf{X}_b - \mathbf{X}_{tr})(\mathbf{X}_b - \mathbf{X}_{tr})^T} \\ &\approx \overline{(\mathbf{X}_b - \overline{\mathbf{X}_b})(\mathbf{X}_b - \overline{\mathbf{X}_b})^T}, \end{aligned}$$

and

$$\begin{aligned} \mathbf{P}_a &= \overline{(\mathbf{X}_a - \mathbf{X}_{tr})(\mathbf{X}_a - \mathbf{X}_{tr})^T} \\ &\approx \overline{(\mathbf{X}_a - \overline{\mathbf{X}_a})(\mathbf{X}_a - \overline{\mathbf{X}_a})^T}, \end{aligned}$$

where $\overline{\mathbf{X}}$ denotes the ensemble mean.

As proposed by Evensen (1994, 2003), perturbations are added to the observations in order to implement the EnKF, and serve to maintain variability in the ensemble because the covariance estimates are biased low due to the finite size of the ensemble. A matrix \mathbf{X} is used to hold all ensemble members: $\mathbf{X} = \{x_1, x_2, \dots, x_n\} \in \prod^{n \times N}$, where N is the number of ensemble members and n is the size of the model state vector. Given ensemble mean $\overline{\mathbf{X}}$, the ensemble perturbation matrix can be obtained as:

$$\mathbf{X}' = \mathbf{X} - \overline{\mathbf{X}}. \quad (2.2.1)$$

The ensemble covariance matrix $\mathbf{P}_f \in \prod^{n \times n}$ can be defined as:

$$\mathbf{P}_f = \mathbf{X}' (\mathbf{X}')^T / (N - 1). \quad (2.2.2)$$

Given a vector of observation $d \in \prod^m$, where m is the number of measurements, we can define the N vectors of the perturbed observations as:

$$\mathbf{D} = \{d_1, d_2, \dots, d_N\} \in \prod^{m \times N},$$

where

$$d_j = d + \varepsilon_j, \quad j = 1, \dots, N. \quad (2.2.3)$$

The ensemble of mean-zero observation perturbations can also be stored in the matrix:

$$\gamma = (\varepsilon_1, \varepsilon_2, \dots, \varepsilon_N) \in \prod^{m \times N}. \quad (2.2.4)$$

Then, we can construct the ensemble representation of the measurement error covariance matrix:

$$\mathbf{R}_e = \gamma \gamma^T / (N - 1). \quad (2.2.5)$$

Based on Eq. (2.1.1) and using definitions of the ensemble error covariance matrices in (2.2.5) and (2.2.2), the analysis can be expressed as:

$$\begin{aligned} \mathbf{X}_a = & \mathbf{X} + \mathbf{X}' \mathbf{X}'^T \mathbf{H}^T (\mathbf{H} \mathbf{X}' \mathbf{X}'^T \mathbf{H}^T + \\ & \gamma \gamma^T)^{-1} (\mathbf{D} - \mathbf{H} \mathbf{X}). \end{aligned} \quad (2.2.6)$$

Evensen (2003) introduced an efficient way to solve Eq. (2.2.6) for a large m (number of observations) with a singular value decomposition (SVD) method, assuming the ensemble perturbation and observational error are uncorrelated.

2.3 Ensemble Adjustment Kalman Filter (EAKF)

The EAKF is derived as a Monte Carlo approximation to the nonlinear filter without perturbing observations (Anderson, 2001). It is assumed that the prior ensemble forecast distribution can be represented by a Gaussian distribution with covariance $\hat{\mathbf{P}}_f$ and mean $\hat{\mathbf{X}}_b$ where $\hat{\mathbf{X}}_b = (\mathbf{X}_b, \mathbf{Y})$ is the joint state consisting of both the state and observations. The mean and covariance of the updated ensemble is

$$\hat{\mathbf{X}}_a = \mathbf{P}_f [(\hat{\mathbf{P}}_f)^{-1} \hat{\mathbf{X}}_b + \mathbf{H}^T \mathbf{R}^{-1} \mathbf{H} \mathbf{Y}], \quad (2.3.1)$$

$$\mathbf{P}_f = [(\hat{\mathbf{P}}_f)^{-1} + \mathbf{H}^T \mathbf{R}^{-1} \mathbf{H}]^{-1}. \quad (2.3.2)$$

In order to get the updated ensemble, a linear operator \mathbf{S} is applied to the prior ensemble

$$\hat{\mathbf{X}}_{a,i} = \mathbf{S}^T (\hat{\mathbf{X}}_{b,i} - \hat{\mathbf{X}}_b) + \hat{\mathbf{X}}_a, \quad i = 1, \dots, N, \quad (2.3.3)$$

where $\hat{\mathbf{X}}_{b,i}$ and $\hat{\mathbf{X}}_{a,i}$ are individual members of the prior and updated i th ensemble members of the joint states. A method for computing the appropriate \mathbf{S} can be found in Anderson (2001).

2.4 Ensemble Square Root Filter (EnSRF)

Whitaker and Hamill (2002) described the EnSRF, which conducts a set of parallel data assimilation cycles without perturbed observations. In the EnSRF,

the update for the ensemble mean (denoted by an overbar) and the deviation of the i th ensemble member from the mean is separated:

$$\overline{\mathbf{X}}_a = \overline{\mathbf{X}}_b + \mathbf{K} (\mathbf{Y} - \mathbf{H} \overline{\mathbf{X}}_b), \quad (2.4.1)$$

$$\mathbf{X}'_{a,i} = \mathbf{X}'_{b,i} - \tilde{\mathbf{K}} \mathbf{H} \mathbf{X}'_{b,i}. \quad (2.4.2)$$

Here, \mathbf{K} is the traditional Kalman gain matrix as mentioned in section 2.1 and $\tilde{\mathbf{K}}$ is a ‘‘reduced’’ gain matrix used to update deviations from the ensemble mean:

$$\tilde{\mathbf{K}} = \left(1 + \sqrt{\frac{\mathbf{R}}{\mathbf{H} \mathbf{P}_f \mathbf{H}^T + \mathbf{R}}} \right)^{-1} \mathbf{K}. \quad (2.4.3)$$

The modified Kalman gain matrix is derived to obtain the correct analysis-error covariance with unperturbed observations, and is reduced in magnitude relative to the traditional Kalman gain.

2.5 Ensemble Transform Kalman Filter (ETKF)

According to Bishop et al. (2001), the ETKF represents the forecast error covariance matrix by forecast perturbation: $\mathbf{P}_f = \mathbf{Z}_f (\mathbf{Z}_f)^T$, where $\mathbf{Z}_f = (1/\sqrt{k-1}) \mathbf{X}_f$, $\mathbf{X}_f = (x_{f,1} - \bar{x}_f, x_{f,2} - \bar{x}_f, \dots, x_{f,k} - \bar{x}_f)$, $x_{f,i}$ ($i = 1, 2, \dots, k$) are the k -ensemble forecasts and $\bar{\mathbf{X}}_f$ is the ensemble mean. To obtain the analysis ensemble perturbations, forecast ensemble perturbations \mathbf{X}_f , are subjected to a linear transformation via a \mathbf{T} matrix so that the distribution of the transformed ensemble perturbations matches the Kalman filter expression for the analysis error covariance:

$$\begin{aligned} \mathbf{P}_a = & \mathbf{P}_f - \mathbf{P}_f \mathbf{H}^T (\mathbf{H} \mathbf{P}_f \mathbf{H}^T + \mathbf{R})^{-1} \mathbf{H} \mathbf{P}_f \\ = & \mathbf{X}_f \mathbf{T} \mathbf{T}^T \mathbf{X}_f^T. \end{aligned} \quad (2.5.1)$$

The minimum error variance state estimates based on the standard Kalman filter equation is given by

$$\begin{aligned} \overline{\mathbf{X}}_a = & \overline{\mathbf{X}}_f + \mathbf{P}_f \mathbf{H}^T (\mathbf{H} \mathbf{P}_f \mathbf{H}^T + \mathbf{R})^{-1} (\mathbf{Y} - \mathbf{H} \overline{\mathbf{X}}_f) \\ = & \overline{\mathbf{X}}_f + \mathbf{X}_f [\mathbf{C} \mathbf{T}^{1/2} (\mathbf{T} + \mathbf{I})^{-1} \mathbf{E}^T] \times \\ & [\mathbf{R}^{-1/2} \mathbf{Y} - \mathbf{R}^{-1/2} \mathbf{H} \overline{\mathbf{X}}_f] \end{aligned} \quad (2.5.2)$$

where \mathbf{C} and \mathbf{T} are the eigenvectors and eigenvalues of $\mathbf{X}_f^T \mathbf{H}^T \mathbf{R}^{-T/2} \mathbf{R}^{-1/2} \mathbf{H} \overline{\mathbf{X}}_f$, respectively, and \mathbf{E} contains the eigenvectors of $\mathbf{R}^{-1/2} \mathbf{H} \mathbf{X}_f \mathbf{X}_f^T \mathbf{H}^T \mathbf{R}^{-T/2}$ that are not in the null space of $\mathbf{X}_f \mathbf{X}_f^T$.

The transformation matrix (\mathbf{T}) can then be shown to take the form $\mathbf{T} = \mathbf{C} (\mathbf{T} + \mathbf{I})^{-1/2} \mathbf{C}^T$ so that the normalized analysis ensemble perturbations are given by $\mathbf{X}_a = \mathbf{X}_f \mathbf{T}$ (Bishop et al., 2001). Wang et al. (2004) further developed the ETKF by centering the analysis ensemble perturbations, and reported an improvement in the method.

2.6 Comments on different methods

All ensemble-based Kalman filters described in sections 2.2–2.5 use the ensemble forecasts to estimate the background-error covariance matrix \mathbf{P}_f and produce an ensemble of analyses. However, it should be noted that the EnKF assimilates perturbed observations rather than the observations themselves. The algorithm updates each ensemble member with a different set of observations perturbed with random noise Eq. (2.2.3). Because randomness is introduced in every assimilation cycle, the update is considered stochastic. All of the other three methods (EAKF, EnSRF and ETKF) do not add stochastic noise to the observations. They are all called deterministic algorithms (Hamill, 2006). Tippett et al. (2003) commented that these deterministic analysis ensemble updates are the implementations of Kalman square root filters. Due to the non-uniqueness of the deterministic transformation used in square root Kalman filters, as showed in sections 2.3–2.5, three methods (EAKF, EnSRF and ETKF) use different ways to update the ensemble perturbations.

3. Numerical experiments and results

The Lorenz-63 model is used as a test bed to examine the above ensemble Kalman filters in strongly nonlinear dynamics. One of the most challenging aspects of it is an intermittent regime change from one basin of attraction to another, where each basin forms one of the wings of the butterfly-shaped attractor. The regime change is generally difficult to predict. The equations of the model can be written as:

$$\begin{cases} dx/dt = -\sigma(x - y), \\ dy/dt = -xz + \gamma x - y, \\ dz/dt = xy - \beta z, \end{cases} \quad (3.1)$$

where $x(t), y(t)$, and $z(t)$ are the dependent variables, and σ, γ , and β are parameters of the model. We have chosen the following commonly used values for the parameters in the equations: $\sigma = 10, \gamma = 28$, and $\beta = 8/3$. The model is then written in discrete form and integrated using a fourth-order Runge-Kutta time scheme with a time step of $\Delta t = 0.01$.

The initial conditions for the reference (true) state are given by $(x_0, y_0, z_0) = (1.22, 0.412, 20.49)$, which is obtained by integrating the model for an extended period starting from an arbitrary initial condition. To develop a clear demonstration, in this study we examined only one complete trajectory around both wings of the attractor, for a total of 200 time steps, specifying observations 8 times during the first 80 time steps in one phase (wing) of the attractor. Numerical experiments are then performed to quantify whether as-

simulating these “observations” of the state (x, y, z) on one wing (phase) of the butterfly will lead to an accurate forecast of the phase transition and an improved forecast for the other wing (phase) of the attractor.

The observations and the initial conditions to generate ensemble forecasts are simulated by adding normally distributed noise with a zero mean and a standard deviation equal to 1.0 to the reference solution. For the observations, the variables x, y and z are measured at 8 observational times. For the data assimilation experiments, an ensemble of 20 members provides the sample of the background and analysis distributions. Figure 1 shows a single orbit of the reference (true) state, observations, the ensemble and the ensemble mean when no data assimilation is performed. The ensemble serves as the first guess for the data assimilation experiments. As shown in Fig. 1, the ensemble mean of the guess fields is far away from the reference state, indicating the sensitivity of phase-transition predictions to small perturbations.

The aforementioned four ensemble Kalman filters (sections 2.2–2.5) are implemented for the data assimilation experiments. The data assimilation is performed sequentially at each observing time during the first 80 steps. Table 1 shows the Root Mean Square (RMS) errors of the ensemble mean E_1 for different experiments before and after the data assimilation. E_1 is defined as

$$E_1 = \sqrt{\frac{1}{m} \sum_{i=1}^m \left(\frac{1}{n} \sum_{j=1}^n X_{i,j} - X_{i,\text{tr}} \right)^2}, \quad (3.2)$$

where $n = 20$ is the number of ensemble members, $m = 3$ is the number of state variables, $X_{i,j}$ is the j th ensemble member for the i th variable, and $X_{i,\text{tr}}$ is the “true” state from which the observations were sampled. The table compares E_1 for the ensembles of the initial guess fields, for the guess (before data assimilation) and the analysis (after data assimilation) fields averaged over 8 analysis steps. It shows very clearly that the analysis error has been significantly reduced after the data assimilation. However, convergence from different methods varies in terms of the value of E_1 for the analysis in different experiments.

To demonstrate the impact of data assimilation, Fig. 2a shows the ensemble mean of forecasts during steps 81 to 200 from all four experiments, compared with the ensemble mean of the guess fields and the reference (true) state. Notable improvement in forecasts is found: all experiments with ensemble Kalman filters predict the phase transition of the nonlinear system. Forecast errors are also significantly reduced.

Experiments are conducted to investigate the sensitivity of the ensemble Kalman filters to observational

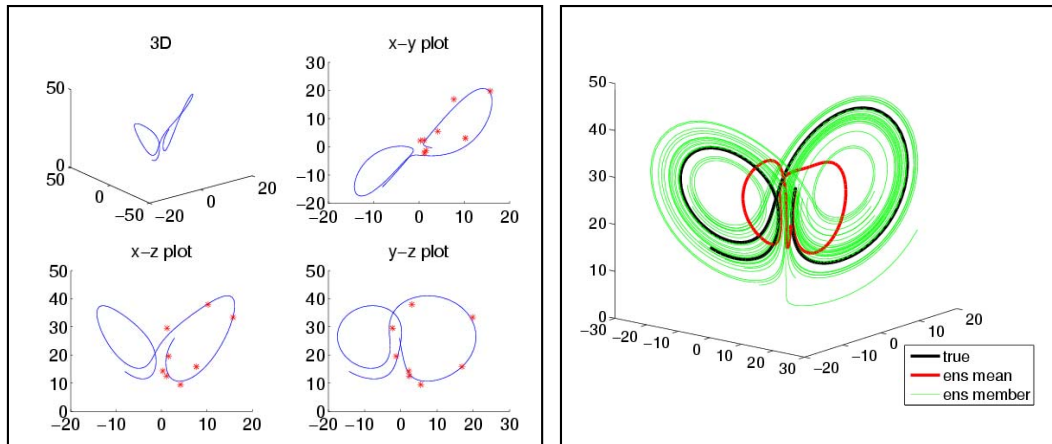


Fig. 1. The left panel shows the reference (true) state (blue curve) and observations (red stars). The right panel presents the true state (black curve), 20 ensemble members of the first guess fields (green curves) and the ensemble mean of the guess fields (red curve).

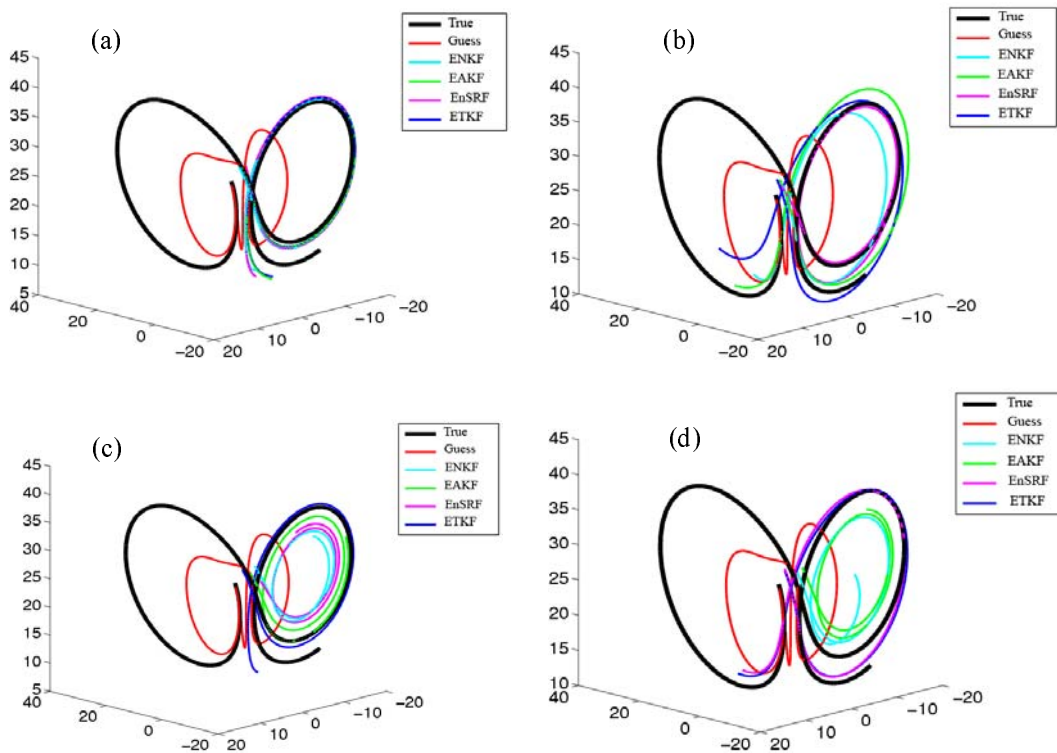


Fig. 2. Sensitivity of ensemble Kalman filters to the observational errors. The figures show the forecasts from the analysis obtained by assimilation of the data with a standard deviation of the errors equal to (a)1, (b)2, (c)3, and (d)5 with different ensemble filters.

Table 1. Comparison of E_1 before and after the analysis for all experiments.

Experiment	E_1 (guess field)	E_1 (Before analysis) Averaged over all analysis steps	E_1 (After analysis) Averaged over all analysis steps
ENKF	3.18	1.918	1.109
EAKF	3.18	1.402	0.949
EnSRF	3.18	1.368	1.239
ETKF	3.18	1.241	0.851

errors. Increased random errors—with the mean of the error equal to 0 and the standard deviation of the errors equal to 2, 3, and 5, respectively—are added to the reference state at the same “observational stations” to generate three additional sets of observations. Data assimilation experiments are repeated with four ensemble Kalman filters using these three sets of observations. Figures 2b, 2c, and 2d show the mean of the ensemble forecasts after data assimilation with each method, compared with the first guess and the reference state. It is apparent from Fig. 2 that all of the methods are sensitive to the levels of observational error. With the increase in observational errors, the forecast error becomes larger and the model tends to fail to predict the phase transition. Even in the case when the standard deviation of the observational errors equals 2 and the forecast errors are small in most of the cases, the phase errors are already seen in the forecasts. When the standard deviation of the observational errors increases to 3 and then 5, significant errors appear in both the forecast and the phase transition for almost all the methods.

Ensemble Kalman filters use the ensemble forecasts to obtain the error covariance of the background fields. They are only optimal in an infinite ensemble. However, a finite ensemble size must be used in real applications because of the computational expense. Therefore, sampling error is present in any ensemble filter data assimilation system. In order to examine the sensitivity of ensemble Kalman filters to the ensemble size used in the data assimilation, additional experiments are also performed with the use of 10, 50, and 100 ensemble members and the results are compared with the experiment using 20 ensemble members. Figure 3 shows the variances of the analysis relative to the reference state averaged over 8 analysis steps, and the variances of the forecasts relative to the reference state. The EnKF method is sensitive to the ensemble size used in data assimilation. The other three methods do not appear as sensitive to the choice of ensemble size.

Sources of background error are various in real cases, and include both sampling errors and errors in the model formulation. Model error is often ignored

because it is difficult to quantify, and sampling error is not explicitly accounted for in the ensemble filter formulation. This results in an under-estimation of the background error covariances. In order to compensate for the sampling error, an inflation factor is often used to multiply to the background covariances and enlarge the background error (Anderson and Anderson, 1999). When properly tuned, the inflation factor can improve the convergence of the analysis during data assimilation. Although the optimal inflation factor should be tuned and may be different for each filter algorithm, we performed a limited set of experiments to examine the sensitivity. Two experiments are completed with inflation factors of 1.02 and 1.05, and the results are

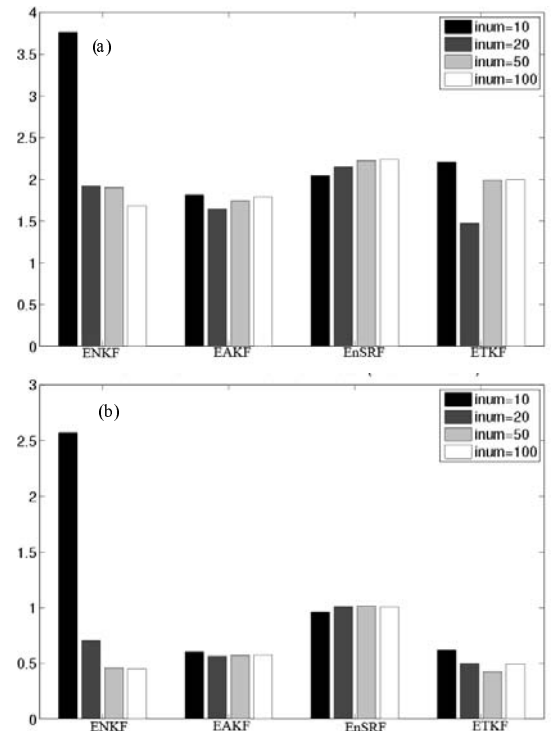


Fig. 3. Sensitivity of ensemble Kalman filters to the ensemble size. The figure shows (a) variances of analysis relative to the reference (true) state and (b) variances of the forecast relative to the true state from four ensemble Kalman filters with the use of 10, 20, 50, and 100 ensemble members.

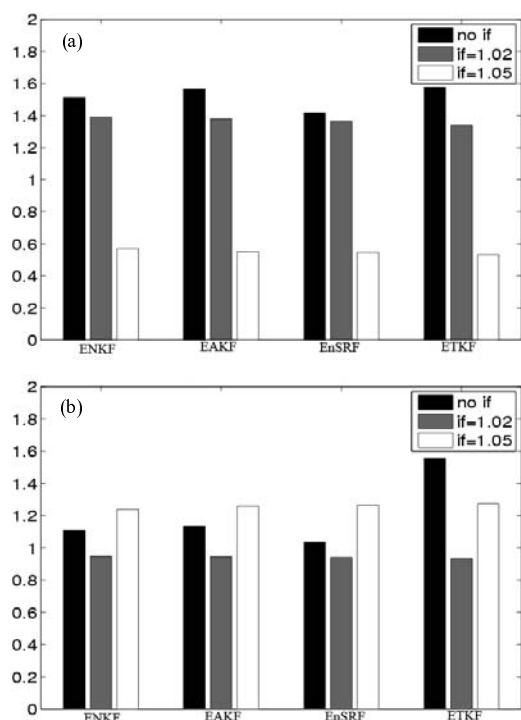


Fig. 4. The impact of an inflation factor on ensemble Kalman filters. The figure illustrates (a) the Root Mean Square (RMS) error of the ensemble mean relative to the observations and (b) the RMS error of the ensemble mean relative to the reference (true) state from four ensemble Kalman filters with an inflation factor of 1 (without inflation), 1.02 and 1.05.

compared with the previous experiment without the inflation.

Figures 4a and 4b show the root mean square errors of the ensemble mean relative to the observations and the reference state, respectively. Apparently, all of the four ensemble Kalman filters are sensitive to the inflation factor. Specifically, a larger inflation factor causes the analysis results to be closer to the observations, while a smaller inflation factor results in the analysis being relatively farther from the observations. However, since observations are usually not perfect, the larger inflation factor does not always lead to smaller forecast errors. Compared with the experiments without the inflation factor, the inflation factor of 1.05 leads to poorer forecasts in most of the experiments, whereas the inflation factor of 1.02 results in the best forecasts using all of the four ensemble Kalman filters. Therefore, only a properly defined inflation factor will benefit the analysis and forecasts.

4. Summary

In this study, we examined four ensemble Kalman filters in terms of their abilities to analyze and predict

nonlinear dynamics. Although the simple model (e.g., Lorenz, 1963) is used, results still lead us to some useful conclusions. Specifically, it is found that:

(1) Ensemble-based Kalman filters can help improve the prediction of the nonlinear dynamics during the phase transition;

(2) All methods are sensitive to observational errors; when observational errors become larger, the forecast of the nonlinear system tends to be more uncertain. However, different filters may have different abilities to tolerate the observational errors;

(3) Accuracy of the analysis depends on the size of the ensemble in the analysis cycle, and in order to achieve the same accuracy, one method may require a smaller ensemble size than another;

(4) Phase transition prediction skill is sensitive to the magnitude of the inflation factor, implying that sampling error may be present in those experiments.

This study has proven that ensemble Kalman filters are a useful tool for atmospheric data assimilation in the presence of nonlinearity. Results pointed out a number of factors we must consider in real applications. However, since the real cases could be much more complicated than the simple model presented in this study, conclusions from this study will be further confirmed with more advanced modeling systems in future work.

Acknowledgements. The authors would like to express their appreciation to Drs. J. Anderson and X. Wang for useful discussion. The authors are also grateful to three anonymous reviewers for their review comments that are helpful for improving this manuscript. The first author is supported by U.S. National Science Foundation through Award Number ATM-0833985.

REFERENCES

- Anderson, J. L., 2001: An ensemble adjustment Kalman filter for data assimilation. *Mon. Wea. Rev.*, **129**, 2884–2903.
- Anderson, J. L., and S. L. Anderson, 1999: A Monte Carlo implementation of the nonlinear filtering problem to produce ensemble assimilation and forecasts. *Mon. Wea. Rev.*, **127**, 2741–2758.
- Bishop, C. H., B. J. Etherton, and S. J. Majumdar, 2001: Adaptive sampling with the ensemble transform Kalman filter. Part I: Theoretical aspects. *Mon. Wea. Rev.*, **129**, 420–436.
- Evensen, G., 1994: Sequential data assimilation with a non-linear quasi-geostrophic model using Monte Carlo methods to forecast error statistics. *J. Geophys. Res.*, **10**, 143–162.
- Evensen, G., 2003: The ensemble Kalman filter: Theoretical formulation and practical implementation. *Ocean Dynamics*, **53**, 343–367.

- Hamill, T. M., 2006: Ensemble-based atmospheric data assimilation. *Predictability of Weather and Climate*. T. Palmer and R. Hagedorn, Eds., Cambridge University Press, 124–156.
- Houtekamer, P. L., and H. L. Mitchell, 1998: Data assimilation using an ensemble Kalman filter technique. *Mon. Wea. Rev.*, **127**, 1378–1379.
- Lorenz, E. N., 1963: Deterministic nonperiodic flow. *J. Atmos. Sci.*, **20**, 130–141.
- Miller, R. N., M. Ghil, and F. Gauthiez, 1994: Advanced data assimilation in strongly nonlinear dynamical systems. *J. Atmos. Sci.*, **51**, 1037–1056.
- Tippett, M. K., J. L. Anderson, C. H. Bishop, T. M. Hamill, and J. S. Whitaker, 2003: Ensemble square root filters. *Mon. Wea. Rev.*, **131**, 1485–1490.
- Verlaan, M., and A. W. Heemink, 2001: Nonlinearity in data assimilation applications: A practical methods for analysis. *Mon. Wea. Rev.*, **129**, 1578–1589.
- Wang, X., C. H. Bishop, and S. J. Julier, 2004: Which is better, an ensemble of positive-negative pairs or centered spherical simplex ensemble? *Mon. Wea. Rev.*, **132**, 1590–1605.
- Whitaker, J. S., and T. M. Hamill, 2002: Ensemble data assimilation without perturbed observation. *Mon. Wea. Rev.*, **130**, 1913–1924.